HIGHLIGHTS FROM THE NA61/SHINE EXPERIMENT*

Antoni Marcinek

for the NA61/SHINE Collaboration

Institute of Nuclear Physics Polish Academy of Sciences, Kraków, Poland

Received 15 August 2022, accepted 29 August 2022, published online 14 December 2022

The NA61/SHINE experiment is a fixed-target, broad acceptance facility at the CERN SPS. This contribution summarizes the most recent results from the strong interactions NA61/SHINE programme and presents news on the detector upgrade in preparation for the future data taking. The strong interactions programme consists in a two-dimensional scan in beam momentum (from 13A to 150A/158A GeV/c, $\sqrt{s_{NN}}$ from 5.1 to 17.3 GeV) and system size ($p+p$, Be+Be, Ar+Sc, Xe+La reactions). The experiment searches for the second-order critical end-point in the temperature *versus* baryo-chemical potential phase diagram and studies the properties of the onset of deconfinement discovered by its predecessor, NA49 at the CERN SPS. The presented results include K/π multiplicity ratios as a function of energy and system size, singly and multi-strange hadron production in $p+p$ reactions, multiplicity and net-charge fluctuations measured by higher order moments in $p+p$, Be+Be, and Ar+Sc collisions, proton and charged hadron intermittency in Ar+Sc and Pb+Pb reactions, HBT measurements in Ar+Sc, and collective electromagnetic effects in Ar+Sc collisions.

DOI:10.5506/APhysPolBSupp.16.1-A8

1. Introduction

The NA61/SHINE experiment at the CERN SPS owes its name (SPS Heavy Ion and Neutrino Experiment) to a two-fold experimental programme. On the one hand, it conducts precise spectra measurements necessary for cosmic ray and neutrino experiments. On the other, it investigates the onset of deconfinement (OD) discovered by its predecessor, the NA49 experiment at the CERN SPS [1] and searches for the critical point (CP) of the strongly interacting matter.

The latter part of the programme, the strong interactions programme, is the subject of the present paper. Within it, NA61/SHINE performed a two-dimensional scan of system size and collision energy (Fig. 1, left).

* Presented at the 29$^{\text{th}}$ International Conference on Ultrarelativistic Nucleus–Nucleus Collisions: Quark Matter 2022, Kraków, Poland, 4–10 April, 2022.

This corresponds to scanning the phase diagram of the strongly interacting matter [2] (Fig. 1, right). It should be noted that due to the search for CP, which involves fluctuation variables, it is paramount to minimize system volume fluctuations and, consequently, the experiment focuses mainly on central collisions. Hence, the system size scan as opposed to the more usual centrality scan.

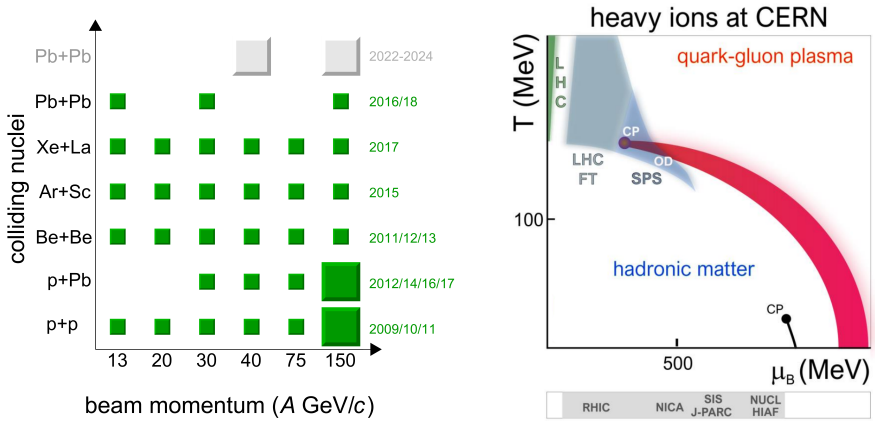

Fig. 1. NA61/SHINE system size and energy scan performed within the strong interactions programme (left) and the phase diagram of the strongly interacting matter (right) studied in this scan.

2. Identified hadron spectra in Be+Be and Ar+Sc collisions

The published, new results on identified hadron spectra in Be+Be collisions [3] and preliminary results on identified hadron spectra in Ar+Sc collisions are discussed in detail in Ref. [4]. Figure 2 shows the summary of these studies, the system size and energy dependence of the K^+/π^+ ratio in midrapidity. A pronounced 'horn' in the Pb+Pb/Au+Au collisions, associated with the OD [5], is clearly visible. There are, however, some unexpected features in this dependence. First, the $p+p$ collisions do not follow a smooth increase with energy, but rather an abrupt change of the trend at SPS energies. Second, the Be+Be collisions feature similar K^+/π^+ ratio values to $p+p$, while the Ar+Sc collisions have no horn structure, but at the top SPS energy converge to similar (large) ratio values as the Pb+Pb collisions. These two observations can be attributed [6], respectively, to two transitions between domains of dominance of specific hadron production mechanisms: from *hadron resonances* to *strings* when changing collision energy for small systems and from *strings* to *QGP fireball* (onset of fireball) when changing system size at large energies. These new NA61/SHINE data allow for the first time to sketch such a diagram of high-energy nuclear collisions and emphasize how important the SPS energy range is.

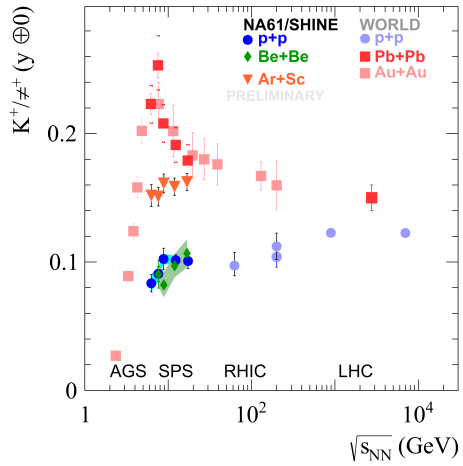

Fig. 2. System size and energy dependence of the K^+/π^+ ratio in midrapidity [4] including published, new NA61/SHINE results for Be+Be [3] and preliminary Ar+Sc collisions.

3. Search for the critical point

Preliminary results on multiplicity fluctuations of charged hadrons and net-charge fluctuations of charged hadrons, measured as the ratios of cumulants [7] of the order up to 4, are shown, respectively, in Fig. 3 and Fig. 4. No structure indicating the CP is visible. While κ_4/κ_2 ratio is consistent for all measured systems, interesting system size dependence is observed for multiplicity κ_2/κ_1 and net-charge κ_3/κ_1 ratios. In the first case, there is an increasing difference in collision energy between small systems ($p+p$ and

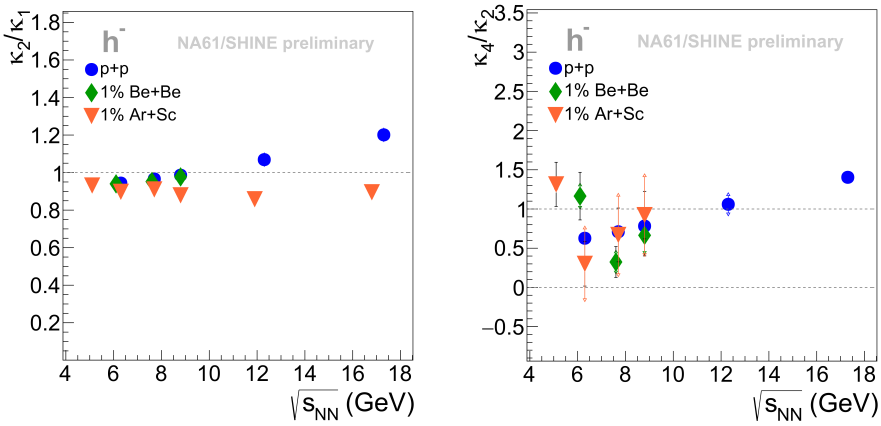

Fig. 3. Preliminary results on the system size and energy dependence of the multiplicity fluctuations for negatively charged hadrons.

Be+Be) and the Ar+Sc system. In the second case, there is a difference between the Be+Be and other systems, again increasing with $\sqrt{s_{NN}}$. Work is still ongoing to get more data points for Be+Be and Ar+Sc systems.

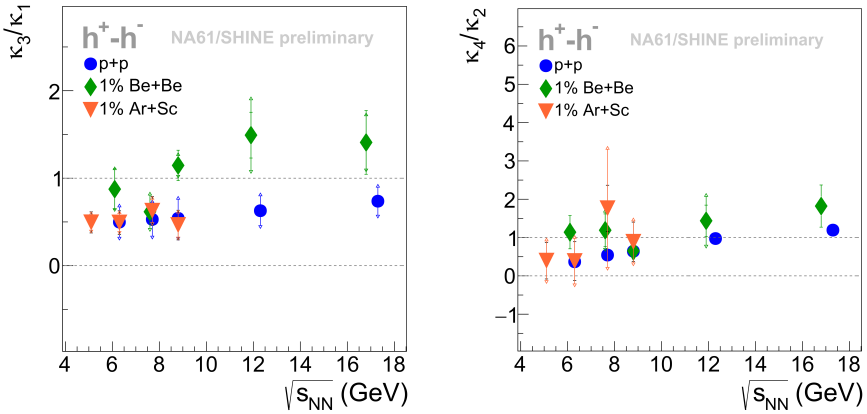

Fig. 4. Preliminary results on the system size and energy dependence of the net-charge fluctuations for charged hadrons.

Another phenomenon frequently associated with the critical point of strongly interacting matter is intermittency. In this analysis, the transverse momentum space in midrapidity is divided into cells in which particles are counted to calculate scaled factorial moments F. For the system experiencing critical behaviour, the theory predicts [8] specific power-law scaling of the moment of the order r as a function of the number of cells M: $F_r(M) \sim M^{\phi_r}$. Figure 5 shows preliminary results on the proton intermittency in the central Ar+Sc and Pb+Pb collisions at, respectively, 150A GeV/c and 30A GeV/c

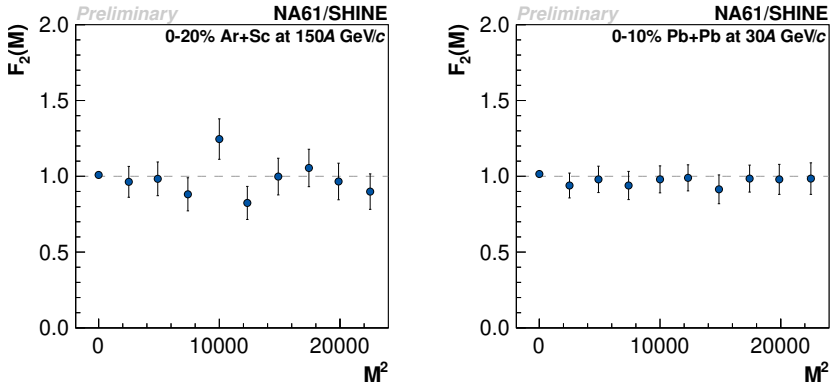

Fig. 5. Preliminary results on the midrapidity proton intermittency for 0–20% most central Ar+Sc collisions at 150A GeV/c beam momentum (left) and 0–10% most central Pb+Pb collisions at 30A GeV/c beam momentum (right).

beam momenta. Figure 6 shows results for charged hadron intermittency in central Pb+Pb collisions at 30A GeV/c beam momentum up to the fourth scaled factorial moment. These analyses feature statistically-independent points and instead of the (p_x, p_y) cells, cumulative variables are used to remove dependence of the moments on the momentum distribution [9]. While no indication of the critical point is visible in these analyses, a considerable progress is presently being accomplished in order to provide a more advanced methodology, more sensitive to intermittency in the presence of sizeable non-critical background [10].

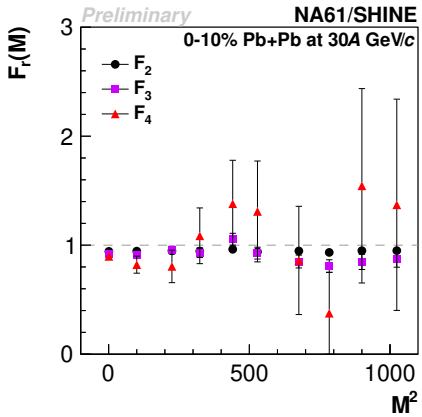

Fig. 6. Preliminary results on the midrapidity charged hadron intermittency for 0–10% most central Pb+Pb collisions at 30A GeV/c beam momentum.

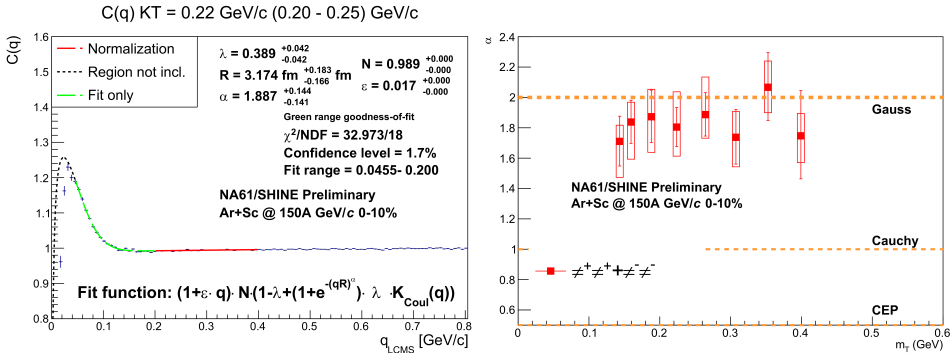

Fig. 7. Preliminary results on the symmetric Levy HBT correlations for the same-charge pion pairs in central Ar+Sc collisions at 150A GeV/c beam momentum. The left plot shows an example fit of the correlation function and the right one shows the dependence of the fitted source shape parameter on the transverse mass of the pair.

The last CP-related results are the symmetric Levy HBT correlations for the same-charge pion pairs in the central Ar+Sc collisions at 150A GeV/c beam momentum shown in Fig. 7. Here, instead of a usual Gaussian source shape, a more general Levy-stable distribution is used. Its parameter α describes the shape of the source: for $\alpha = 2$, the source is Gaussian, for $\alpha = 1$, we have a Cauchy distribution, and the 3D Ising model with a random external field predicts $\alpha = 0.5 \pm 0.05$ for a critical system. From the plot, it is clear that there is no indication of the CP for the central Ar+Sc collisions at the top SPS energy.

4. Spectator-induced electromagnetic effects in Ar+Sc collisions

Figure 8 shows for the first time ever, observation of spectator-induced electromagnetic effects in peripheral small systems (Ar+Sc collisions) at the CERN SPS. The effect is visible as a depletion of the π^+/π^- ratio for small transverse momenta and pion rapidities close to the beam rapidity. Even at intermediate centrality, *i.e.* with a small spectator system, the effect is strong

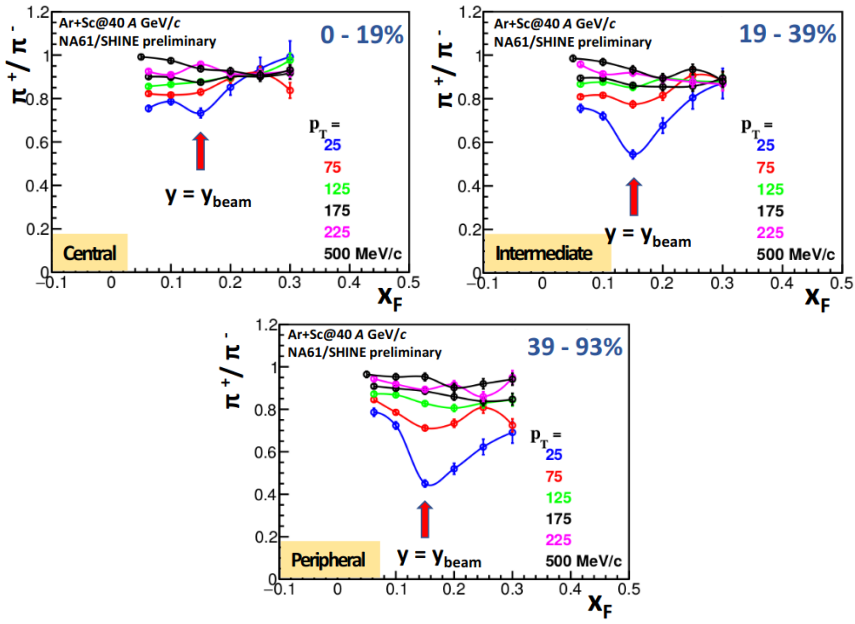

Fig. 8. Preliminary measurements of the spectator-induced electromagnetic effects visible as a depletion of the π^+/π^- ratio for small transverse momenta and pion rapidities close to the beam rapidity for the central (top, left), intermediate (top, right), and peripheral (bottom) Ar+Sc collisions at 40A GeV/c beam momentum. Top right corners of each plot indicate approximate centrality percentiles.

enough to break isospin symmetry. Spectator-induced electromagnetic effects provide information on the space-time evolution of the system [11], partially complementary to femtoscopy.

5. New data on hadron spectra in $p + p$ reactions

The new results on hadron spectra in $p + p$ collisions are also discussed in more detail in Ref. [4]. Here only two most recent results on rapidity spectra of neutral kaons are presented in Fig. 9: the $K^*(892)^0$ at 40 and 80A GeV/c beam momenta [12] compared to 158A GeV/c [13] and the K^0_S at 158A GeV/c compared to model predictions [14]. These data will, on the one hand, serve as a reference for future data from larger systems and, on the other hand, serve as input to models, which struggle to describe the strangeness production at SPS energies. The latter is visible in the right plot of Fig. 9.

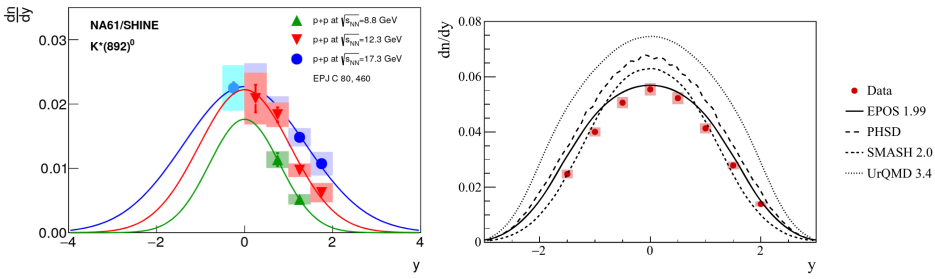

Fig. 9. New results on rapidity spectra of neutral kaons in $p + p$ collisions: the $K^*(892)^0$ at 40 and 80A GeV/c beam momenta [12] compared to 158A GeV/c [13] (left), the K^0_S at 158A GeV/c compared to model predictions [14] (right).

6. Hardware upgrade and future measurements

All of the above results were possible thanks to the versatility of the NA61/SHINE detector system. The spectrometer based on large-volume time projection chambers (TPC) features large acceptance covering the full forward hemisphere down to $p_T = 0$. The latter is feasible due to the fixed-target setup and the magnetic field oriented perpendicular to the beam direction. During the CERN Long Shutdown 2, the whole system underwent an upgrade including the construction of a new Vertex Detector, new Beam Position Detectors, new Time-of-Flight detectors, larger forward calorimeter (Projectile Spectator Detector), new trigger, and data acquisition system and most importantly replacement of the TPC read-out electronics to increase the data rate tenfold to 1 kHz.

The upgrade was necessary to perform the first ever open charm measurement at the SPS energies, which is the main goal of NA61/SHINE data taking in the years 2022–2024 (Fig. 1, left, grey boxes). The latter is motivated by 3 questions:

— What is the mechanism of open charm production?
— How does the onset of deconfinement impact open charm production?
— How does the formation of quark–gluon plasma impact J/ψ production?

In order to answer these questions, it is necessary to know the full phase-space production of $c\bar{c}$ pairs, for which model predictions vary by 2 orders of magnitude [15].

This work was supported by the Polish Minister of Education and Science (contract No. 2021/WK/10).

REFERENCES

[1] NA49 Collaboration (C. Alt *et al.*), *Phys. Rev. C* **77**, 024903 (2008).
[2] F. Becattini, J. Manninen, M. Gazdzicki, *Phys. Rev. C* **73**, 044905 (2006).
[3] NA61/SHINE Collaboration (A. Acharya *et al.*), *Eur. Phys. J. C* **81**, 73 (2021).
[4] M. Lewicki, *Acta Phys. Pol. B Proc. Suppl.* **16**, 1-A66 (2023), this issue.
[5] M. Gazdzicki, M.I. Gorenstein, *Acta Phys. Pol. B* **30**, 2705 (1999).
[6] E. Andronov, M. Kuich, M. Gaździcki, arXiv:2205.06726 [hep-ph].
[7] https://mathworld.wolfram.com/Cumulant.html
[8] N.G. Antoniou, F.K. Diakonos, A.S. Kapoyannis, K.S. Kousouris, *Phys. Rev. Lett.* **97**, 032002 (2006).
[9] A. Bialas, M. Gazdzicki, *Phys. Lett. B* **252**, 483 (1990).
[10] N. Davis, poster presented at the Quark Matter 2022 Conference, Kraków, Poland, 4–10 April, 2022, not included in the proceedings., https://indico.cern.ch/event/895086/timetable/
[11] V. Ozvenchuk *et al.*, *Phys. Rev. C* **102**, 014901 (2020).
[12] NA61/SHINE Collaboration (A. Acharya *et al.*), *Eur. Phys. J. C* **82**, 322 (2022).
[13] NA61/SHINE Collaboration (A. Aduszkiewicz *et al.*), *Eur. Phys. J. C* **80**, 460 (2020).
[14] NA61/SHINE Collaboration (A. Acharya *et al.*), *Eur. Phys. J. C* **82**, 96 (2022).
[15] A. Aduszkiewicz, Technical Report CERN-SPSC-2018-008, SPSC-P-330-ADD-10, CERN, Geneva, March 2018.